

Miniaturized IPD bandpass filter with controllable transmission zero based on modified lumped T-section

Yanzhu Qi | Yazhi Cao | Bo Yuan  | Shichang Chen  | Gaofeng Wang 

MOE Engineering Research Center of Smart Microsensors and Microsystems, School of Electronics and Information, Hangzhou Dianzi University, Hangzhou, China

Correspondence

Yazhi Cao, MOE Engineering Research Center of Smart Microsensors and Microsystems, School of Electronics and Information, Hangzhou Dianzi University, Hangzhou, China.
Email: caoyazi@hdu.edu.cn

Funding information

Zhejiang Provincial Key Research & Development Project,
Grant/Award Number: 2021C01041;
National Key Research and Development Program of China under Grant,
Grant/Award Number: 2019YFB2205003

Abstract

In this letter, a miniaturized bandpass filter (BPF) with controllable transmission zero (TZ) based on one lumped T-section is proposed. To enhance rejection in the BPF, a modified T-section circuit is introduced to generate a controllable TZ that can be readily adjusted by the LC values. To validate the performance, the proposed BPF is fabricated using integrated passive device technology on silicon. The measurement results show that the achievable bandwidth covers 2.4–2.5 GHz, with an insertion loss less than 2.6 dB and a measured return loss less than -15 dB. The fabricated BPF has a compact size of $1.3 \text{ mm} \times 0.8 \text{ mm}$ (i.e., $0.0113 \lambda_0 \times 0.0069 \lambda_0$). The simulated and measured results of the BPF are in reasonably good agreement.

KEYWORDS

band pass filter (BPF), integrated passive device (IPD), transmission zero

1 | INTRODUCTION

A compact bandpass filter with high-frequency selectivity and low insertion loss has the potential to significantly enhance the performance of wireless communication systems. Especially with the increasing miniaturization of communication terminals, on-chip filter is an attractive choice to achieve high integration of the wireless system.¹ Consequently, there has been extensive research on developing high-performance and miniaturized filters in recent years.^{1–10}

A novel synthesis method for lumped-element bandpass filters is proposed in Chen et al.,¹ and A design methodology for optimized minimum inductor bandpass filter (BPF) is presented in Taslimi and Mouthaan.² In addition, a glass-integrated passive device bandpass filter using synthesized stepped impedance resonators is presented in Tseng et al.³ However, all their proposed designs are mainly designed to verify their filter synthesis methods, so the filters performance such as the size and

insertion loss cannot be effectively controlled. Filters designed with differential transformer structures can achieve very compact size,⁴ but its design structure is special and not universal. To improve the out-of-band rejection of the filter, adding transmission zero (TZs) to the filter is an effective method.^{5–7} In Xu et al.,⁵ the paper utilizes the coupling matrices to design a compact low-temperature cofired ceramic (LTCC) bandpass filter which introduces TZs at both sides of the filter passband to enhance the selectivity. In Zhao et al.,⁶ TZs are generated by stepped-impedance stubs to obtain high selectivity. Because the above designs are fabricated on the LTCC technology, their size are also slightly larger. In addition to adding TZs to filter, increasing the filter order is also an effective way to improve the filter. In Lyu et al.,⁸ the design employs a stepped impedance multi-mode resonator to design a high-order on-chip wideband bandpass filters and achieves the wide stopband and high stopband rejection. In Liu et al.,⁹ a BPF based on three π -type units has the advantage of the ultra-wide stopband

due to the nonperiodic phase of the unit. Although the above two designs have wider out-of-band rejection and their passband bandwidth is also wider, there are still challenging to implement them into Wi-Fi, Bluetooth, or 5 G applications. Another way to improve out-of-band rejection is to add an additional filter circuit.^{10–12} In Marin et al.,¹⁰ a TZ is introduced to improve out-of-band rejection by adding low-pass pi-type circuits to the input and output ports of the filter. However, since the design uses a PCB structure rather than an on-chip design. In the design of on-chip filters,^{11,12} a Pi-section circuit is designed so that a TZ is obtained at the upper sidebands, which effectively improving the high-frequency out-of-band rejection performance of the filter.

In this letter, a miniaturized silicon-based IPD BPF is presented. To improve out-of-band rejection, a TZ is produced at lower sidebands. A modified T-section circuit is introduced and analyzed to generate and control this TZ. It can be readily adjusted by LC value in the T-section. Finally, the simulation results from the electromagnetic (EM) simulator and the measured results are shown and compared. The proposed BPF demonstrates competitive overall performance when compared to recently reported works, such as those in Chen and Colleagues.^{1,5,8,9,11,12}

2 | FILTER DESIGN AND ANALYSIS

2.1 | Lumped high-pass T-section circuit for BPF

As shown in Figure 1A, a typical high pass filter is composed of three components, that is, a series capacitor CT1, a shunt inductor LT, and a series capacitor CT2. The cut-off frequency is set to 2.5 GHz, and these values can be calculated by the traditional Chebyshev high-pass filter synthesis method. The values are listed as: CT1 = 1.45 pF, CT2 = 1.45 pF, and LT = 5.3 nH. However, this filter has poor out-of-band rejection due to its low order. A modified lumped T-section circuit is proposed to improve the out-of-band rejection, as shown in Figure 1B. Compared with the conventional lumped T-section circuit, an additional capacitor named CT is attached in series to the shunt inductor LT, which is used to create a TZ. The transmission zero frequency is calculated by

$$f_{TZ} = \frac{1}{2\pi\sqrt{L_T C_T}}. \quad (1)$$

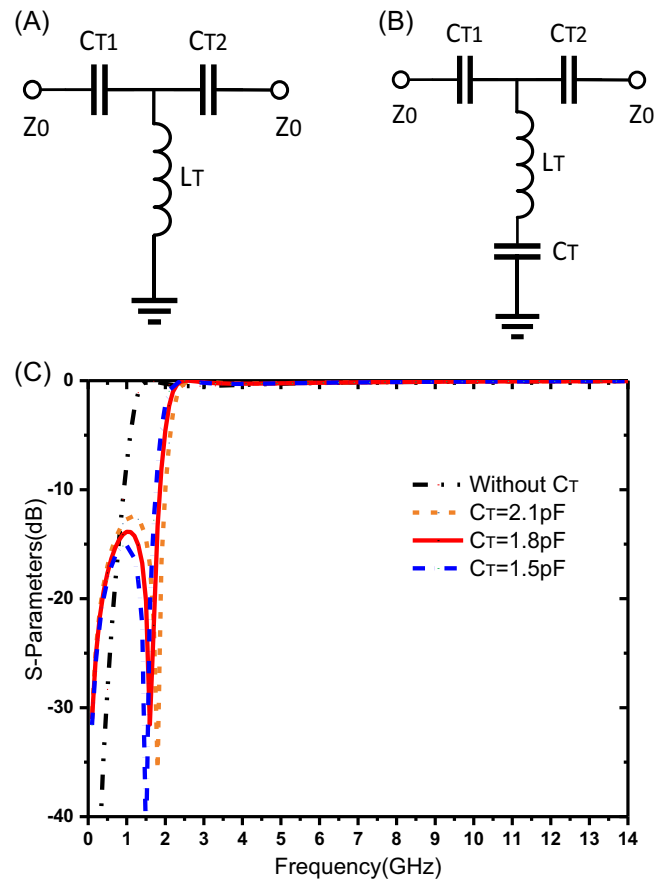


FIGURE 1 Lumped T-section circuit for the TZ and its simulated result. (A) Conventional lumped T-section circuit. (B) Proposed modified lumped T-section circuit. (C) Simulated frequency response curves of the modified lumped T-section circuits with changed values C_T .

As shown in Figure 1C, to validate such a proposed idea, the comparison of simulations with or without C_T is carried out. The classic high pass filter circuit has poor out-of-band suppression because it has no TZ. Meanwhile, a TZ can be generated by the proposed T-Section and the TZ can be controlled by the capacitor C_T . As the value of capacitor C_T increases from 1.5 to 2.1 pF, the TZ position moves from 1.6 GHz to 1.5 GHz. Therefore, the T-section can effectively improve out-of-band suppression.

2.2 | Proposed BPF circuit topology and its performance

The proposed third-order Chebyshev filter topology based on the modified lumped T-section circuit is shown in Figure 2, where Y_0 is $1/50 \Omega$. In addition to the T-section, the other part of the circuit structure is

a third-order Chebyshev filter. The bandwidth of proposed BPF is mainly determined by the topology of the third-order Chebyshev. All the initial element values are calculated by the bandpass filter synthesis method.¹³

Based on the technique described above, the modified filter circuit topology is proposed by high-pass T-section circuit and Chebyshev BPF. Two parts are connected in series, the modified T-Section can introduce a transmission zero on the basis of the Chebyshev BPF to improve the low-frequency out-of-band suppression of the filter. The insertion loss of the filter is reduced by replacing a fixed width inductance with a variable width inductance with a high Q value.¹⁴ Then, the values of the complete BPF circuit are further optimized, and the final values (@2.5 GHz) are shown in Table 1. Based on the synthesized

device values, the device layout is generated, followed by device layout and interconnection. The final layout is shown in Figure 3. Finally, the device values are optimized, and the final layout simulation results are shown in Figure 4B.

3 | FABRICATION AND EXPERIMENTAL RESULTS

The proposed IPD BPF design is fabricated using the thin-film process technology on high resistivity silicon substrate and measured to evaluate its performance. The BPFs were fabricated with a relatively constant value of 11.9, a thickness of 200 μm, and a conductivity of 4000 Ω-cm. To achieve high conductivity, two Cu layers with a thickness of 3 μm each were utilized. Additionally, a thick layer with a relative constant of 7 and a loss tangent of 0.004 was employed as the dielectric layer for the MIM capacitor. Figure 4A shows the final layout of the fabricated BPF chip with the size of 1.3 mm × 0.8 mm, that is, 0.0113 λ₀ × 0.0069 λ₀. This BPF is simulated by UltraEM¹⁵ and is measured by on-wafer probing using the Keysight N5244A PNA-X vector network analyzer and Cascade summit-11000 probe station.

The simulated and measurement results of the proposed BPF are shown in Figure 4B. The good agreement between simulated and measured results is clearly observed. It should be noted that compared to the test results, two zeros were not generated at 5.4 and 10 GHz in the schematic design. The main reason for these two zeros is the tight layout of the structure, and the parasitic effect of inductors L1 and LT with the ground ring produces two zeros. Specifically, at the operating frequency band (2.4–2.5 GHz), it achieves an insertion loss lower than 2.6 dB and a return loss lower than -15 dB. A new TZ is generated at 1.7 GHz to enhance the lower band rejection of the proposed BPF. In addition, the filter has an out-of-band rejection of 20 dB at 0.76 and 1.97 times the center frequency respectively, and better than 30 dB up to six times of the center frequency. There exists some minor frequency shift between the simulated and measured results mainly due to the fabrication tolerance. Comparing to the previous designs as shown in Table 2, it can be observed that the proposed BPF has more compact size compared with other designs. The proposed filter has lower insertion loss compared with Chen et al.¹ And the proposed filter can achieve better frequency selection compared with other references in Table 2.

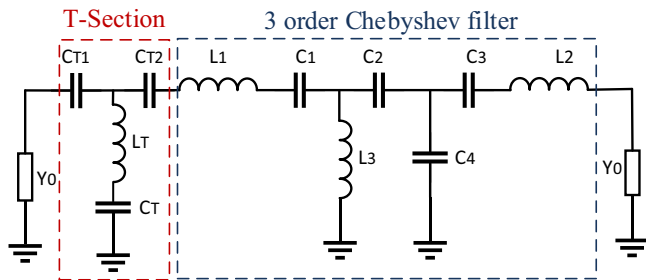


FIGURE 2 Proposed 3th order Chebyshev BPF Circuit topology.

TABLE 1 Values for LC components are shown in Figure 3.

CT1	CT2	CT	C1	C2	C3
1.23	0.42	1.04	1.14	2.5	2.85
C4	LT	L1	L2	L3	Unit: pF, nH
1.4	9.95	15.4	3.11	10.29	

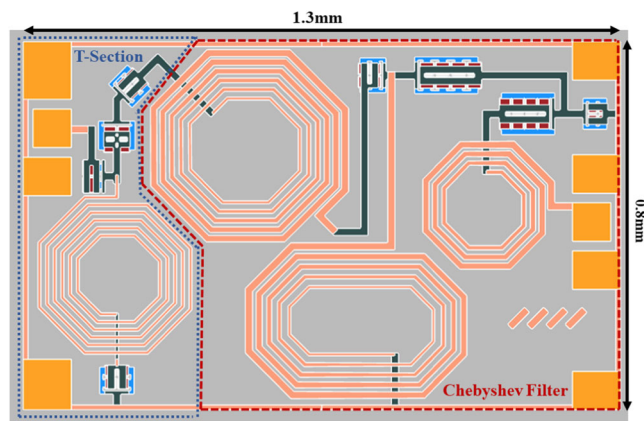


FIGURE 3 Layout of proposed Chebyshev BPF.

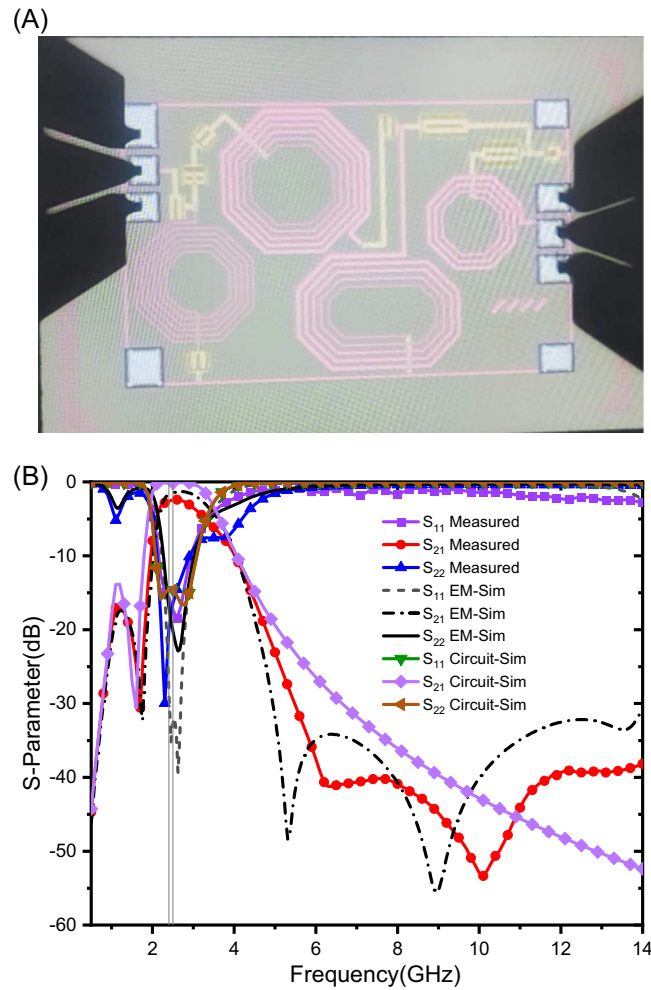


FIGURE 4 (A) Image of the fabricated bandpass filter (BPF). (B) Simulation and measured results of the proposed BPF.

TABLE 2 Comparison of the proposed bpf with other recent works.

References	f_0 (GHz)	Insertion loss (dB)	FBW	Size (λ_0^2) $\times 10^{-4}$	Process
[1]	3	3.1	20%	1.55×0.92	GaAs
[5]	2.6	2.47	10%	1.73×1.473	LTCC
[8]	3	1.15	143%	2.15×0.9	GaAs
[9]	4	2.12	111%	3.2×0.8	GaAs
[11]	3.35	2.05	56.7%	2.0×0.8	GaAs
[12]	3	1.77	66%	1.63×0.62	GaAs
This work	2.45	2.6	38.8%	1.13×0.69	HRS

Abbreviations: FBW, fractional bandwidth, 3 dB bandwidth; λ_0 , the wavelength in air at f_0 ; HRS, high resistivity silicon.

4 | CONCLUSION

In this letter, a miniaturized IPD BPF based on a modified T-section circuit was proposed. The proposed design was designed to enhance rejection of the BPF by

generating a controllable transmission zero at lower sidebands. It can be readily adjusted using the LC value in the modified T-section circuit. The proposed BPF was fabricated on a high-resistivity silicon substrate. The measured results of the fabricated BPF demonstrated a

good agreement with the simulated results. The BPF exhibits a bandwidth covering the range of 2.4–2.5 GHz, with an insertion loss less than 2.6 dB and a measured return loss less than -15 dB. Additionally, the filter can achieve an impressive out-of-band rejection better than 30 dB up to six times the center frequency. Furthermore, the fabricated BPF has a compact size of $1.3 \text{ mm} \times 0.8 \text{ mm}$ (i.e., $0.0113 \lambda_0 \times 0.0069 \lambda_0$). the proposed BPF with superior performances, especially the compact size and low insert loss, is a promising candidate for potential applications of Wi-Fi and Bluetooth communication systems.

ACKNOWLEDGMENTS

This work was supported by National Natural Science Foundation of China under Grant 62141409, National Key Research and Development Program of China under Grant 2019YFB2205003, and Zhejiang Provincial Key Research & Development Project under Grant 2021C01041.

DATA AVAILABILITY STATEMENT

Data sharing not applicable to this article as no data sets were generated or analysed during the current study.

ORCID

Bo Yuan  <http://orcid.org/0000-0001-5045-7584>

Shichang Chen  <http://orcid.org/0000-0003-1628-5429>

Gaofeng Wang  <http://orcid.org/0000-0001-8599-7249>

REFERENCES

- Chen F-J, Cheng X, Zhang L, Tian Y-L, Tang Y, Deng X-J. Synthesis and design of lumped-element filters in GaAs technology based on frequency-dependent coupling matrices. *IEEE Trans Microw Theory Tech.* 2019;67(4):1483-1495.
- Taslimi A, Mouthaan K. Design of optimized minimum inductor bandpass filters. *IEEE Trans Microw Theory Tech.* 2017;65(2):484-495.
- Tseng Y-C, Ma T-G. On-chip GIPD bandpass filter using synthesized stepped impedance resonators. *IEEE Microw Wirel Compon Lett.* 2014;24(3):140-142.
- Li Y, Wang C, Kim N-Y. Design of very compact bandpass filters based on differential transformers. *IEEE Microw Wirel Compon Lett.* 2015;25(7):439-441.
- Xu J-X, Zhang XY, Zhao X-L, Xue Q. Synthesis and implementation of LTCC bandpass filter with harmonic suppression. *IEEE Trans Compon Packag Manuf Technol.* 2016;6(4):596-604.
- Zhao W, Wu Y, Yang Y, Wang W. LTCC bandpass filter chips with controllable transmission zeros and bandwidths using stepped-impedance stubs. *IEEE Trans Circuits Syst II: Express Briefs.* 2022;69(4):2071-2075.
- Wu W-J, Yuan B, Zhao W-S, Wang G. On-chip miniaturized bandpass filter using gallium arsenide-based integrated passive device technology. *Microw Opt Technol Lett.* 2022;64:688-693.
- Lyu Y-P, Zhou Y-J, Zhu L, Cheng C-H. Compact and high-order on-chip wideband bandpass filters on multimode resonator in integrated passive device technology. *IEEE Electron Device Lett.* 2022;43(2):196-199.
- Liu B-G, Zhou Y-J, Cheng C-H. Miniaturized ultra-wideband bandpass filter with ultra-wide stopband using π -type unit with inductive loading on integrated passive device. *IEEE Trans Circuits Syst II: Express Briefs.* 2021;68(11):3406-3410.
- Marin S, Martinez JD, Valero CI, Boria VE. Microstrip filters with enhanced stopband based on lumped bisected Pi-sections with parasitics. *IEEE Microw Wirel Compon Lett.* 2017;27(1):19-21.
- Luo X-H, Cheng X, Zhang L, et al. A miniaturized on-chip BPF with ultrawide stopband based on lumped Pi-section and source-load coupling. *IEEE Microw Wirel Compon Lett.* 2019;29(8):516-519.
- Jiang Y, Feng L, Zhu H, et al. Bandpass filter with ultra-wide upper stopband on GaAs IPD technology. *IEEE Trans Circuits Syst II: Express Briefs.* 2022;69(2):389-393.
- Cameron RJ, Kudsia CM, Mansour RR. *Microwave Filters for Communication Systems: Fundamentals, Design and Applications.* Wiley; 2007:136-170.
- Vanukuru VNR, Chakravorty A. High-Q characteristics of variable width inductors with reverse excitation. *IEEE Trans Electron Devices.* 2014;61(9):3350-3354.
- UltraEM V202109*, Faraday Dynamics, Inc., 2022.

How to cite this article: Qi Y, Cao Y, Yuan B, Chen S, Wang G. Miniaturized IPD bandpass filter with controllable transmission zero based on modified lumped T-section. *Microw Opt Technol Lett.* 2024;66:e34134. doi:10.1002/mop.34134